X-ray extended-range technique for precision measurement of the X-ray mass attenuation coefficient and Im(f) for copper using synchrotron radiation

C.T. Chantler [a,*], C.Q. Tran [a], D. Paterson [a], D. Cookson [b], Z. Barnea [a]

[a] *School of Physics, University of Melbourne, Melbourne, Victoria 3010, Australia*
[b] *ANSTO, Private Mail Bag 1, Menai, NSW 2234 and Chem-Mat-CARS-CAT (Sector 15, Bldg 434D), Argonne National Laboratory, 9700 S. Cass. Avenue, Argonne, IL 60439, USA*

Abstract

We reconsider the long-standing problem of accurate measurement of atomic form factors for fundamental and applied problems. We discuss the X-ray extended-range technique for accurate measurement of the mass attenuation coefficient and the imaginary component of the atomic form factor. Novelties of this approach include the use of a synchrotron with detector normalisation, the direct calibration of dominant systematics using multiple thicknesses, and measurement over wide energy ranges with a resulting improvement of accuracies by an order of magnitude. This new technique achieves accuracies of 0.27–0.5% and reproducibility of 0.02% for attenuation of copper from 8.84 to 20 keV, compared to accuracies of 10% using atomic vapours. This precision challenges available theoretical calculations. Discrepancies of 10% between current theory and experiments can now be addressed. © 2001 Elsevier Science B.V. All rights reserved.

PACS: 78.20.Ci; 32.80.Cy; 78.70.Dm; 78.20.Bh

1. Introduction

X-ray diffraction and medical transmission imaging have been major scientific developments following the first X-ray attenuation investigation by Röntgen. Quantum mechanical determination of atomic form factors has combined with the dynamical theory of X-ray diffraction to allow quantitative prediction of X-ray interactions. By the 1970's, this work had yielded tabulations of X-ray scattering from all ele-ments, complemented by a large body of experimental literature [1–4]. Recent major developments have concentrated on applications for structural determination near absorption edges, including the use of Bijvoet ratios [5], multiple-wavelength anomalous dispersion (MAD) techniques [6], X-ray absorption fine structure (XAFS) investigations [7] and diffraction anomalous fine structure (DAFS) [8].

Methods for experimentally determining the fundamental atomic form factor have included X-ray interferometry [9,10], reflection and refraction [11, 12], diffraction intensities [13,14] and pendellösung fringes [15,16], with developing efforts at synchrotron facilities over the last two decades. These innovative

---

* Corresponding author.
 E-mail address: chantler@ph.unimelb.edu.au (C.T. Chantler).

approaches have been complemented by more traditional investigations of linear attenuation to provide experimental values for the complex atomic form factor over an extensive range of X-ray energies.

Every attenuation experiment is, in principle, of simple design. An absorbing sample is inserted into the beam and the difference in the transmitted signal is measured as a function of energy. The Beer–Lambert law allows extraction of a mass attenuation coefficient, and an assumption regarding scattering is made to derive from it the imaginary component of the form factor Im(f). Traditional attenuation measurements in studies over three decades have claimed accuracies of 1%. It has also been claimed that, even in ideal experiments, absolute accuracies below 1% were unlikely to be achieved.

Many theoretical issues have been raised in the past decades. Differentiation between alternative relativistic correction factors for Re(f), the separability of the scattering coefficients, the use of Dirac–Hartree–Fock or Hartree–Slater wavefunctions with or without a normalisation correction, and the independent particle assumption are all key issues for isolated atom computations in atomic physics. Computations investigating these issues theoretically find differences varying from 1% to 10% or more. Hence an experimental accuracy of 0.5% should be able to distinguish between wavefunction and orbital precision using alternate computational techniques for neutral systems, and to probe solid state and resonant atomic physics near edges.

2. Difficulties with theory and experiment

Previous high-precision experimental investigations [17–19] have raised concerns about particular implementations of theory. Recent tabulations of theoretical results are discrepant from one another by up to 10σ across energy ranges for a range of elements [20,21].

Critical experimental compilations and syntheses show inconsistencies of 10–30% in regions of interest. Most applications using atomic wavefunctions or X-ray form factors have relied upon one selected theoretical tabulation with convergence to 1% but with variation from alternate theory by ten times this value. Such uncertainties cast doubt upon issues such as the determinations of structural details and electron density redistribution due to bonding. The experimental variability implies that significant undiagnosed systematics are limiting results and their consequent interpretations.

Experimental inconsistencies suggest that most previous work reports the experimental self-consistency while not accounting for several key systematic contributions in the final error budget. Sample characterisation is crucial in that the local thickness must be determined to high accuracy to avoid systematic errors of several percent. Harmonic contamination and inadequate X-ray monochromation typically lead to underestimates of the true attenuation coefficient [22]. Invalid assumptions regarding coherent and inelastic scattering lead to significant error for high energies. Detector non-linearities and beam instabilities introduce time- and flux-dependent systematic effects. Previous experiments using relative energies calibrated by reference to a local X-ray edge may be affected by chemical shifts and inadequately determined. Synchrotron experiments of this type are often subject to beam drifts in position and energy.

Most experimental work reported previously used a single foil. Single-foil measurements are limited in their ability to observe harmonic contributions, detector non-linearity and scattering, and have a large uncertainty in thickness determination at low energy and for high-Z materials where the foil used is only a few microns thick. Single-foil techniques may yield precise results while providing an inaccurate determination of the attenuation due to the presence of these systematics. Measurements made using anode sources often only use one sample. XAFS measurements at synchrotrons also use only a single foil sample.

If this summary list of potential problems is complete, then one of the key problems, and one of the key novelties of this work, is the design of an experimental method which is either insensitive to these systematics or allows these systematic contributions to be accurately determined. This work identifies contributing experimental systematics and describes a method for obtaining high-accuracy measurements of the mass attenuation coefficient and hence of the imaginary component of the atomic form factor. This Letter focuses on copper as one of the most carefully investigated substances and one of the primary benchmarks of the International Union of Crystallography attenuation project [20].

3. Experimental technique

A sample is interposed between a downstream detector and an upstream beam monitor in an X-ray beam monochromatized by a double-reflection silicon 111 crystal, where second-order harmonics are forbidden and only third-order harmonics may be significant. Two apertures define the beam size of 1 mm × 1 mm with a vertical divergence of 0.12 ± 0.03 mrad. The monochromator is detuned to minimise higher-order harmonic contamination. Between the foil mounting stage and the detector is a wheel on whose rim a series of 20 aluminium foils of widely varying thicknesses are mounted. Different thicknesses of aluminium can thus be introduced into the beam by rotation of the wheel. The aluminium foils are then used to measure harmonic contamination and detector non-linearity to 0.03%. In general, higher-order harmonic contamination can be a serious problem for accurate measurement; see, for example, [23], where limitations in accuracy due to inadequate monochromation were emphasised. However, in this work, no measurable harmonic signature or non-linearity above 0.03% was observed.

Simultaneous measurements were made of the downstream detector signal and the upstream monitor signal with the sample interposed, and with the sample absent, so attenuation of X-rays by the air path, window absorption and air scattering naturally cancels. All detector readings are corrected for the electronic offset noise (dark current) of the amplifiers measured when no X-rays pass through the detectors.

This experiment was based at the ANBF station in Tsukuba, Japan. Synchrotron measurements are an improvement over the use of laboratory sources, where low flux limits the final precision and accuracy. We directly investigated the distribution of signals with time to quantify systematics, since fluctuations at a synchrotron occur on several timescales [24]. These fluctuations, from several independent sources, can be isolated and quantified, so that the limiting precision can be reduced to a very low level [25]. As a result, observed standard deviations of intensity ratios of 0.01–0.02% across the full range of energies show excellent reproducibility.

Energies were calibrated to 1–3 eV accuracy using diffraction patterns of NIST standard powders (Si640b ($a_0 = 5.430940(11)$ Å) and LaB$_6$ ($a_0 =$

4.15695(6) Å)) with lattice spacings calibrated to the wavelength standard. These powders exhibited no orientational specificity. The accuracy was confirmed by the agreement between measurements using each powder standard at 11 energies. The residual energy uncertainty is a minor contribution to the final error, except in the immediate vicinity of the K-edge XAFS structure, where small changes in energy correspond to significant changes in attenuation.

The X-ray extended range technique combines normalisation, including offsets, with investigation of statistical noise contributions and optimisation of correlation. The technique requires measurements using multiple samples satisfying an attenuation criterion, direct investigations of contributing systematics over a wide energy range, and direct calibration of attenuator thicknesses, which is the greatest remaining source of inaccuracy.

In this work, three foils of different thicknesses were used for each energy, covering an extended attenuation criterion given by $0.5 < \ln(I_0/I) < 6.0$ [26,27]. For a given exposure, this prescription yields a similar precision for each foil if the detectors are linear and statistical noise dominates. The foils are changed regularly with changing energy so that the criterion is satisfied. The method of replacing absorbers is aided by a three-sample stage to allow fully automated and remote control of this operation, and to allow the thickness of the sample region exposed to the beam to be calibrated with respect to the other samples to 0.01%. Using multiple foils for each energy allows other limitations due to non-linearities, harmonics, correlation and non-statistical noise to be quantified. The detailed method for addressing these concerns has been discussed above and in the associated references.

The sensitivity and accuracy of these investigations require measurement of absolute photon energies and mass attenuation coefficients over an extended range of energies. This is the key to the quantitative determination of systematics.

4. Absolute determination of column thickness using the X-ray extended range technique

In addition to statistical optimisation, direct analysis of linearity and harmonics, and calibration of energy, the X-ray extended range technique calibrates

the thickness of thin samples against those of thick samples of the same element and purity. Thin samples are required to satisfy the attenuation criterion at lower energies. Thick samples are needed for high energies. The mechanical accuracy with which thin sample thicknesses can be measured is usually poor, and thin samples are usually highly variable in their local thickness compared to their average thickness.

By conducting the experiment across a wide range of energy, the column thickness ρt exposed to the beam for thin samples can be calibrated against that of the thicker samples exposed to the beam at an appropriate intermediate energy, so a 5 μm Cu sample used in a low energy measurement is calibrated in situ to 0.1% against a 100 μm thick Cu sample. This technique therefore improves the accuracy of measurements for the lower (9 keV) X-ray energies by a factor of twenty. The achievement of this improvement requires the use of multiple samples for each energy, and requires the measurement of attenuation over an extended energy range. By comparison, accuracies of atomic vapour measurements have been limited to 10% by the uncertainty of the integrated column density.

The determination of ρt remains the dominant limitation to the accuracy of the final mass attenuation coefficients in our experiments. A measurement of mass and area gives the average value of this to high accuracy (0.06%). We make a detailed X-ray profiling of the surface structure and relative attenuation over the surface area in 1 mm × 1 mm grids. This mapping of the local variations of thickness over the surface area gives the local thickness at the region in the X-ray beam path relative to the average. The accuracy decreases in this step due to the surface structure and the limited precision of the mapping, but still yields a final accuracy at the highest energies (20 keV) of 0.27%. In part, this high accuracy is due to the high fluxes and hence statistical precision possible at the synchrotron. The calibration of the local thickness of thinner samples is made by direct comparison of the log of the attenuation ratios, at energies where both the reference sample and the thinner sample satisfy the attenuation criterion. This thickness 'transfer' increases the percentage error in accuracy but is much lower than the error on using the thicker sample at low energies or the error on using the thin sample in isolation. For our lowest energy (9 keV) this increases

the uncertainty only marginally, to 0.33% of the thickness.

5. Application to copper

High-Z impurities in copper, typically due to silver and lead, yield a maximum correction less than 0.013% for the samples discussed. Oxidation on the surface of order 3.5 nm [11] leads to a correction less than 0.02% for the thinnest (5 μm) samples.

The Beer–Lambert law relates strictly to photoelectric absorption excluding coherent and incoherent scattering. In fact, in our experiments, when a sample is inserted, the upstream monitor shows an increase in the flux of 0.1–0.2% as a function of energy. This signal is consistent with modelling based on Rayleigh scattering and fluorescence. However, this scattering showed no net effect on the experimental values of $[\mu/\rho]$ larger than 0.02%.

The final accuracy of measured mass attenuation coefficients is thus limited to 0.3%. Near the K-edge the energy uncertainty makes a further contribution. The photoelectric absorption coefficient $[\mu/\rho]_{pe}$ and the imaginary component of the atomic form factor $\mathrm{Im}(f)$ require the subtraction of the contribution from scattering due to the mass scattering coefficient $[\sigma/\rho]$:

$$[\mu/\rho]_{pe} = [\mu/\rho]_{observed,\ total}$$
$$- [\sigma/\rho]_{coherent+incoherent}.$$

An experimental upper limit to scattering is given by the backscattering signal, consistent with Rayleigh scattering and not consistent with Laue–Bragg diffraction peaks. In this experiment where scattering contributions for copper are small and primarily due to Rayleigh scattering, theory may be used to subtract off these contributions, with an estimated uncertainty equal to half the difference between major tabulations. This then subtracts 0.5% ± 0.075% of the total mass attenuation coefficient for energies just above the K-edge or 2.1% ± 0.15% at 20 keV [2,21]. The uncertainty in this correction is not dominant, and adds no uncertainty to measurement of $[\mu/\rho]_{total}$ or to the *relative* structure of $\mathrm{Im}(f)$ over wide energy ranges.
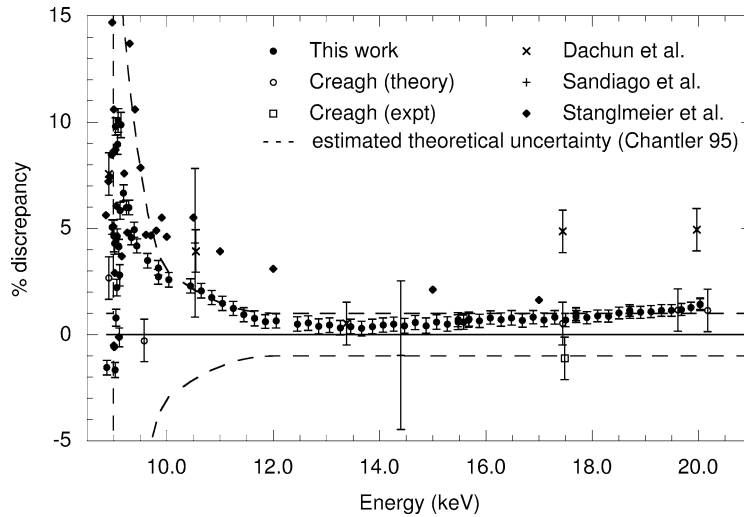
Fig. 1. Comparison between this work and existing data; absolute calibration of energies against NIST reference standards. Data is plotted relative to theory [21] (% = $([\mu/\rho] - [\mu/\rho]_{theory})/[\mu/\rho]_{theory}$) with an estimation of uncertainty in theory given by the region between dashed lines. This comparison is identical to that for discrepancies of $Im(f) = [\mu/\rho]uAE/2hcr_e$ [21]. An alternate theory [20] agrees with the reference theory. Agreement with latest theory is good. Error bars of theory increase to 20% near the K-edge. Current data compared to earlier results [11,29,30].

6. Results

We determine $Im(f)$ to be 3.8 ± 0.013 e/atom (electrons/atom) at 9 keV and 1 ± 0.003 e/atom at 20 keV, compared to corresponding theoretical values of 3.8 ± 0.38 e/atom and 1.00 ± 0.01 e/atom [21]. This sensitivity in electrons per atom enables critical investigation of large contributions to $Im(f)$ from atomic or bound near-edge resonances (XANES), local X-ray absorption fine structure (XAFS) and small relativistic 0.1 e/atom contributions to the real component of the atomic form factor. Recent speculation has suggested the possibility of atomic XAFS (AXAFS), at the level of 0.05 e/atom [28] in $Im(f)$, well above our sensitivity of 0.01 e/atom contributions. Investigation of AXAFS will, however, depend upon better atomic theory calculations, as computations are sensitive to small variations of the shape of the atomic orbital wavefunctions.

Our results are summarised in Fig. 1. Our data is in reasonable agreement with the 1.0% uncertainty of theory of Chantler [21] away from the K-edge. Theoretical uncertainty increases near the edge. Comparison of our experimental results with theoretical calculations shows discrepancies in the region of the edge,

but also in the 16–20 keV range (see Fig. 1). The plotted experimental data obtained using laboratory sources [29,30] show significant discrepancies of 4σ and 4% with our results. A further experimental datum [20] lies within 2σ of our results, and has a relatively low quoted error bar. Error contributions of this datum have not been reported. Ref. [11] is a synchrotron measurement with very high statistical precision, but systematic problems of the type discussed have led to major discrepancies with theory and other experimental work.

Both theories [20,21] use Dirac–Hartree–Fock wavefunctions with a Kohn–Sham potential and include relativistic corrections. They are both atomic calculations and hence do not allow for nearest neighbour interactions or photoelectron interactions with surrounding electron density (XAFS). This is of course an explanation of part of the discrepancy in the near-edge region, combined with questions of convergence precision in the same region.

Fig. 2 provides a comparison of our absolute measurements with previous relative measurements [31]. The relative measurements were scaled to compare the agreement of the near-edge oscillations observed in the two experiments. The size of the dots representing
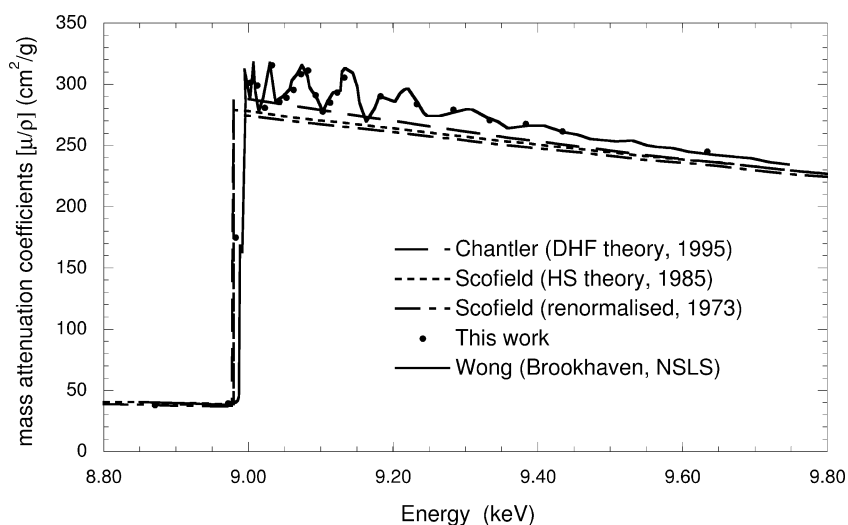
Fig. 2. Detailed XAFS (X-ray anomalous fine structure) measurement at the Cu K-edge on an *absolute* scale, compared to DHF theory (– – –) [21] and earlier theory (- - -) [2]. (●) This work (dot size represents 10σ). The relative observations (—) [31] are in excellent agreement. Theory, based upon the isolated atom approximation, serves as a reference profile for XAFS contributions.

our experimental measurements is increased to 10σ for visibility. XAFS structure is modified by chemical and nearest neighbour interactions, and the structural turning points are used as reference points to investigate chemical processes of many types. Our technique is able to provide absolute values of mass attenuation coefficient and energy for those turning points with high accuracy.

Fig. 2 also provides a more detailed plot in the vicinity of the absorption edge, showing the detailed XAFS (strictly extended XAFS) profile. This also plots the earlier theoretical curve [21] together with two additional theoretical curves using Hartree–Slater wavefunctions with or without relativistic corrections [2].

A number of authors have made detailed comparisons of their experimental results with Scofield theory, which exists in two forms. The first form (unrenormalised) is based on Hartree–Slater orbitals and hence omits certain relativistic corrections. At some level, this limitation would be expected to yield a lower accuracy, for example, than the self-consistent Dirac–Hartree–Fock approach. For $Z = 2$–54, Scofield provided estimated renormalisation factors to convert to values which might be expected from a relativistic Hartree–Fock model. This correction was based primarily on the sum of component orbital electronic

amplitudes at the nucleus, and so is not equivalent to a fully relativistic procedure (as the discrepancy between Chantler and the renormalised values of Scofield in Fig. 2 illustrates). The differences between renormalised and unrenormalised results vary from 5% to more than 15%.

Scofield's original recommendation was to apply the renormalisation correction in all cases. The renormalisation correction was not based on a Dirac–Hartree–Fock computation but estimated the correction factor for treating the charge density near the nucleus to higher accuracy. Hence this should be a useful correction at high energies for all Z. Some reviewers found that this improved agreement with experiment [32]. A decade-long discussion has concerned itself with the relative validity of the renormalised and unrenormalised calculations of a Schrödinger versus Dirac approach. Review authors have concluded that unrenormalised results were superior [2] or that the experimental result lies between the renormalised and unrenormalised calculations [33]. The last statement implies that theoretical error lies in the region of 5–10%, as opposed to the claimed accuracy of order 0.1–1% at medium energies.

The experimental results for copper in the 8–10 keV region are in much better agreement with DHF
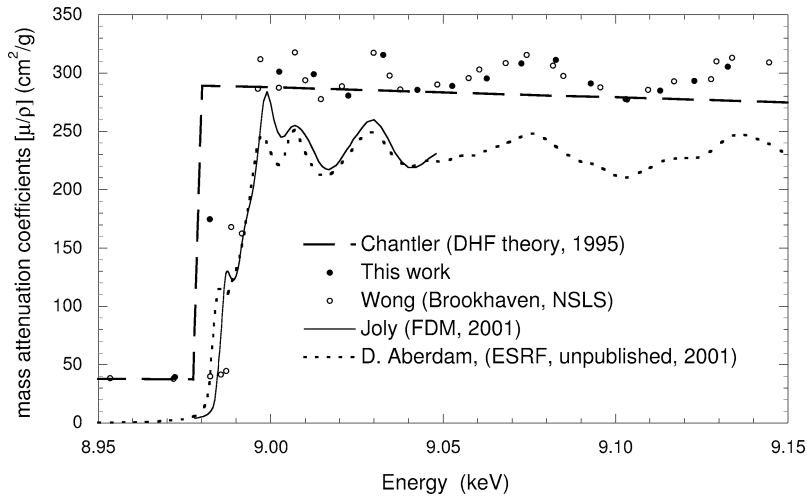
Fig. 3. Detail of the near edge oscillations at the Cu K-edge on an *absolute* scale, compared to recent solid state computations using the FDM technique. (●) This work (dot size represents 10σ). The relative observations are in excellent agreement. Theory based upon the isolated atom approximation, does not explain these near-edge features. Locations of peaks are well represented by theory, but offsets, background levels, and relative amplitudes of peaks need further theoretical investigation.

theory [21] than with Hartree–Slater theory [2]. In the upper energy range, both results are consistent within their uncertainties.

7. Solid state structure

The EXAFS structure illustrated can only be explained by a combination of accurate relativistic atomic and solid state computations. Modelling of these systems has often used an atomic multiplet approach [34], a local density approximation using infinite crystals (a band structure approach) [35–37], or a cluster approach using multiple scattering theory [7,39]. These codes are contemporaneous with the latest general atomic calculations just discussed, but they are qualitative developments for the interpretation of local structure. Often these solid state computations have been limited to muffin-tin averaging of the potential [38], but these restrictions have been lifted in recent years with Koringa–Kohn–Rostoker Green's function methods, various approaches including the full linear augmented plane wave (FLAPW) method, and the finite difference method (FDM) [40,41].

A brief commentary on these methods includes the observations that the more generalized potentials are more able to represent, in a meaningful manner, local disorder, which will be reflected in the near-edge oscillations. A cluster of 13 atoms, additionally, is completely inadequate and will not represent the local structure. The peaks and structure may be fully converged in such cases, but will often be a poor match even compared to the atomic computation using a fully relativistic code.

A specific direct comparison is provided by the latest result from the FDM formalism [42]. This is plotted against the data in Fig. 3 [43]. This does not cover the full range of observed data but concentrates on the near-edge region from -10 to $+60$ eV. The computations have some significant computational cost at energies further away from the edge. Other theoretical predictions (such as the FEFF codes [7]) have greater facility over larger ranges of energy, but there remains significant difficulty in meaningful comparisons outside this range, in part due to the often necessary limitations of experimental data.

From our illustration, it is clear that solid state calculations are extremely relevant and useful in this region, and that many details of the structure are explained by the latest solid state theory. The relative locations of XAFS peaks are well reproduced. It should be remembered that theoretical computations, the rela-

tive calculations of Wong, and unpublished scaled and offset data from ESRF [44] all have a somewhat arbitrary offset in energy, and also most have an offset or scaling correction for the edge jump. The core hole widths in this region convolve any sharp structure or sharp edges of theory and this is also not uniformly implemented for differing computations. Hence we should be comparing relative peak locations of different sources. Only the current work uses an absolute calibration of both energy and attenuation coefficient without offsets or scaling. Other calculations using FLAPW have been reported and also show good agreement with the relative peak locations of the XAFS oscillations [38].

It is clear that the offsets are much more difficult to compute, that far-edge structure and base levels are extremely challenging to estimate using these techniques, and that details of the near-edge oscillations need further theoretical developments. An absolute calibration of the local cross-section is not a trivial result of current solid state theory, although such theory does a very good job with the edge jump, for example. The second and third experimental peak heights appear to be underestimated by theory compared to the first peak, although their location is fairly well-matched.

8. Further discussion and conclusions

The large number and appropriate distribution of our experimental results over the energy range of investigation (8.84–20 keV) is a major advantage in comparison with other results. Our results are among the first of sufficient accuracy to probe and distinguish between alternative theoretical calculations and to quantify solid-state contributions near the Cu Kα edge. In particular, the data provide high-precision profiles of structure while simultaneously giving high-accuracy results, and promise to allow observation of small contributions to near-edge structure (such as AXAFS). The data obtained are relevant for MAD, XAFS and tomographic investigations, in addition to the relevance for mass attenuation coefficient and atomic form factor theoretical and experimental investigations.

Our measurements are more accurate than previous measurements of Im(f). The accuracy exceeds

the quoted theoretical uncertainties of all calculations. The limiting precision for determining relative structure is two orders of magnitude better than that of earlier work. Our technique provides a key to answering questions about orbital wavefunctions, correlations and solid-state resonances.

The X-ray extended range technique is capable of determining relative structure and absolute values of the photoelectric absorption coefficient and the imaginary component of the atomic form factor. This provides a direct window into an orbital-by-orbital transform of the electron density. The technique provides an absolute baseline for the quantitative interpretation of XAFS structure, and can compare such structure with an atomic, isolated atom model to quantitatively investigate atomic resonances and solid state ordering.

In the current experiment, the lower energy results suggest the validity of DHF approaches to determine wavefunctions and form factors rather than the Hartree–Slater method. While this may seem obvious, each method involves a range of different assumptions and convergence issues, and previous experimental results have not been of sufficient accuracy to distinguish between alternatives. The simpler Hartree–Slater method still appears quite reliable in the upper energy range (between 15 and 20 keV). The 'renormalisation' procedure is not useful for this experimental data set.

Detailed solid state theory is required to explain details of the structure and oscillations observed in this experiment, although current experimental data appears to challenge even these approaches relating to absolute calibration, background levels and edge steps, and values well away from edges. Further experiments are invited for energies above 20 keV, where deviations between theory again reach several percent. A finer grid near the edge location with the same absolute accuracy as reported would contribute significantly to solid state investigations and to near-edge XAFS studies.

Acknowledgements

References

[1] D.T. Cromer, D. Liberman, J. Chem. Phys. 53 (1970) 1891.

[2] E.B. Saloman, J.H. Hubbell, J.H. Scofield, At. Data Nucl. Data Tables 38 (1988) 1;
E.B. Saloman, J.H. Hubbell, NBSIR 86-3431 (1986);
J.J. Scofield, LLNL Report UCRI-51326 (1973).

[3] J.H. Hubbell, W.J. Veigele, E.A. Briggs, R.T. Brown, D.T. Cromer, R.J. Howerton, J. Phys. Chem. Ref. Data 4 (1975) 471.

[4] B.L. Henke, E.C. Gullikson, J.C. Davis, At. Data Nucl. Data Tables 54 (1993) 181.

[5] J.M. Bijvoet, Proc. K. Ned. Akad. Wet. B 52 (1949) 313.

[6] W.A. Hendrickson, Science 254 (1991) 51;
L.K. Templeton, D.H. Templeton, Acta Cryst. A 44 (1988) 1045.

[7] J.J. Rehr, R.C. Albers, S.I. Zabinsky, Phys. Rev. Lett. 69 (1992) 3397;
D. Sayers, E. Stern, F. Lytle, Phys. Rev. Lett. 27 (1971) 1204.

[8] H. Stragier, J.O. Cross, J.J. Rehr, L.B. Sorensen, C.E. Bouldin, J.C. Woicik, Phys. Rev. Lett. 69 (1992) 3064.

[9] M. Hart, D.P. Siddons, Proc. R. Soc. London A 376 (1981) 465.

[10] D.C. Creagh, Phys. Lett. 103A (1984) 52.

[11] F. Stanglmeier, B. Lengeler, W. Weber, H. Göbel, M. Schuster, Acta Cryst. A 48 (1992) 626.

[12] M. Deutsch, M. Hart, Phys. Rev. B 30 (1984) 640.

[13] L.K. Templeton, D.H. Templeton, Acta Cryst. A 47 (1991) 414.

[14] Z. Barnea, in: S. Ramaseshan, S.C. Abrahams (Eds.), Anomalous Scattering, Munksgaard, Copenhagen, 1975.

[15] P.F. Price, E.N. Maslen, S.L. Mair, Acta Cryst. A 43 (1987) 183.

[16] P.J.E. Aldred, M. Hart, Proc. R. Soc. London A 332 (1973) 223.

[17] L. Gerward, J. Phys. B 22 (1989) 1963;
J.F. Mika, L.J. Martin, Z. Barnea, J. Phys. C 18 (1985) 5215;
D.C. Creagh, J.H. Hubbell, Acta Cryst. A 43 (1987) 102.

[18] A. v. dem Brone, T. Dohrmann, A. Verweyen, B. Sonntag, K. Godehusen, P. Zimmermann, Phys. Rev. Lett. 78 (1997) 4019.

[19] Y. Azuma, H.G. Berry, D.S. Gemmell, J. Suleiman, M. Westerlind, I.A. Sellin, J.C. Woicik, J.P. Kirkland, Phys. Rev. A 51 (1995) 447.

[20] D.C. Creagh, W. McAuley, in: A.J.C. Wilsons (Ed.), International Table for X-Ray Crystallography, Vol. C, Kluwer Academic, 1995, Section 4.2.6, p. 206;
D.C. Creagh, J.H. Hubbell, in: A.J.C. Wilsons (Ed.), International Table for X-Ray Crystallography, Vol. C, Kluwer Academic, 1995, p. 206, Section 4.2.4, p. 189.

[21] C.T. Chantler, J. Phys. Chem. Ref. Data 24 (1995) 71;
C.T. Chantler, J. Phys. Chem. Ref. Data 29 (2000) 597.

[22] C.Q. Tran, Z. Barnea, M. de Jonge, D. Paterson, D.J. Cookson, C.T. Chantler, J. Synch. Rad., submitted.

[23] D.C. Creagh, J.H. Hubbell, Acta Cryst. A 46 (1990) 402.

[24] C.T. Chantler, C.Q. Tran, D. Paterson, Z. Barnea, D.J. Cookson, X-Ray Spectrum. 29 (2000) 449.

[25] C.T. Chantler, C.Q. Tran, D. Paterson, D.J. Cookson, Z. Barnea, X-Ray Spectrum. 29 (2000) 459.

[26] B. Nordfors, Ark. Fys. 18 (1960) 37.

[27] C.T. Chantler, Z. Barnea, C.Q. Tran, J. Tiller, D. Paterson, Opt. Quantum Elec. 31 (1999) 495.

[28] A. Filiponi, A. DiCicco, Phys. Rev. B 53 (1996) 9466.

[29] W. Dachun, D. Xunliang, W. Xinfu, Y. Hua, Z. Honggyu, S. Xinyin, Nucl. Instrum. Methods B 71 (1992) 241.

[30] T.K.U. Sandiago, R. Gowda, Pramana 48 (1997) 1077.

[31] J. Wong, Reference X-ray spectra of metal foils, EXAFS Materials, Inc., 871 El Cerro Blvd, Danville CA, USA (1999). These results have a very fine grid giving the local structure with greater detail than most published results. This data, after scaling to give absolute results, is excellent for testing structural reproducibility of XAFS.

[32] J.H. Hubbell, I. Verb, J. Phys. Chem. Ref. Data 8 (1979) 69.

[33] L. Gerward, J. Phys. B 22 (1989) 1963;
L. Gerward, NIM B 69 (1992) 407.

[34] F.M.F. De Groot, J. Electron Spectr. Relat. Phenom. 62 (1993) 111;
C. De Nadai, A. Demourges, J. Grannec, F.M.F. de Groot, Phys. Rev. B 63 (2001) 125123.

[35] G. Doolen, D.A. Liberman, Phys. Scr. 36 (1987) 77.

[36] L.F. Mattheiss, R.E. Dietz, Phys. Rev. B 22 (1980) 1663.

[37] D.A. Muller, Ultramicroscopy 78 (1999) 163.

[38] J.E. Muller, O. Jepsen, J.W. Wilkins, Solid State Commun. 42 (1982) 365.

[39] T.A. Tyson, K.O. Hodgson, C.R. Natoli, M. Benfatto, Phys. Rev. B 40 (1989) 947.

[40] P. Rez, J.R. Alvarez, C. Pickard, Ultramicroscopy 78 (1999) 175.

[41] Y. Joly, Phys. Rev. B 53 (1996) 13029.

[42] Y. Joly, Phys. Rev. B 63 (2001) 125120.

[43] Y. Joly, private communication (2001).

[44] D. Aberdam et al., ESRF (2001), unpublished.